Research Square

Preprints are preliminary reports that have not undergone peer review.
They should not be considered conclusive, used to inform clinical practice,
or referenced by the media as validated information.

Emergent chirality-dependent electromotive force in Weyl semimetals enabled by generalized unitary transformation

S. Doshabchi-Ersi
Azarbaijan Shahid Madani University
H Mohammadpour
mhmdpour@azaruniv.ac.ir
Azarbaijan Shahid Madani University
A. Phirouznia
Azarbaijan Shahid Madani University

Article

Keywords: Spin-motive force, Weyl semimetals, Chirality

Posted Date: September 8th, 2026

DOI: https://doi.org/10.21203/rs.3.rs-10710072/v1

License: This work is licensed under a Creative Commons Attribution 4.0 International License.
Read Full License

Additional Declarations: No competing interests reported.

Emergent chirality-dependent electromotive force in Weyl semimetals enabled by generalized unitary transformation

S. Doshabchi-Ersi[1,2], H. Mohammadpour[1,2*], Arash Phirouznia[1,2*†]

[1]Department of Physics, Faculty of Basic Sciences, Azarbaijan Shahid Madani University, 53714-161, Tabriz, Iran.
[2]Condensed Matter Computational Research Lab, Azarbaijan Shahid Madani University, 53714-161, Tabriz, Iran.

*Corresponding author(s). E-mail(s): mhmdpour@azaruniv.ac.ir; Phirouznia@azaruniv.ac.ir;
†These authors contributed equally to this work.

Abstract

The generalized Faraday technique can facilitate the calculation of spin-motive force (SMF) utilizing the unitary transformation framework. However, while the unitary transformation approach can be effectively applied to derive an effective collinear exchange interaction within non-collinear magnetic configurations, its application becomes limited when dealing with Hamiltonians that include other types of spin-dependent interactions. In this research, we have extended the unitary transformation method to encompass systems exhibiting spin-momentum coupling. The results indicate that the exchange interaction between the spins of the conduction electrons and the magnetization of the substrate leads to the generation of a spin motive force which depends on chirality of Weyl fermions, provided that the magnetic domain wall of the substrate layer is in motion.

Keywords: Spin-motive force, Weyl semimetals, Chirality

1 INTRODUCTION

The announcement of topological semimetals has been a valuable achievement for prolonged efforts that have been made for decades to recognize topological quasi particles in condensed matter physics that act in accordance with the same physical laws as elementary particles [1–7]. Weyl semimetals is a prime category of topological semimetals, which provides developing relativistic Weyl fermions in the bulk and Fermi arc surface states link two Weyl points with opposite chirality on the boundary of a bulk sample [6–10]. Basically there is a connection between Weyl and Dirac semimetals. when, either time reversal symmetry or the spatial symmetry breaks in Dirac semimetals, Dirac point splits into two Weyl points of opposite chirality[11–13]. Unique properties of Weyl semimetals like high mobility because of its gapless spectrum, possessing topologically protected Weyl points and spin-momentum locking, have made them to noticeable subject in progressive applications such as spintronics and valleytronics [14, 15]. Exchange interaction between conduction electron spin and magnetization causes two phenomena, spin-transfer torque (STT) and spin-motive force (SMF). Whereas angular momentum transfer is arises between spin current and magnetization by spin transfer torque, spin-motive force is responsible for energy transfer in the system, thus spin-motive force is expected to provoke an important contribution to energy management in future spintronics with low energy consuming applications. Energy-harvesting technology is a principle concept in spintronics and extends a new way in conversion between magnetic and electric energy by usage of magnetic materials, while the SMF introduces that important and basic concept [16].

Although the foundational ideas and theoretical framework of SMF were developed between the 1970s and 1990s, the initial experimental validations did not occur until the late 2000s. This delay was due to the need for precise control of dynamic magnetic textures at submicron meter scales[17–19]. Nanowires were the first samples exhibited spin-motive force that induced by magnetic domain wall motion[20]. Observed

SMFs are commonly $100nV - 1\mu V$ in magnitude in research labs [17–19, 21, 22]. The evolution of the SMF theory in the past decade has enlightened the role of the nonadiabaticity in electron spin dynamics [23–25]. The existence of Dzyaloshinskii-Moriya interaction can amplify the SMF that is generated by the movement of ferromagnetic domain walls induced by an external magnetic field. It has been demonstrated theoretically that a domain wall affected by a Dzyaloshinskii-Moriya interaction can lead to increased spatial rotation of the magnetization, resulting in an enhancement of the SMF [26]. The behavior of magnetization in uneven magnetic arrangements generates a spin-dependent force acting on conduction electrons via s-d coupling. This electric field that arises is referred to as SMF, and it appears in different magnetic configurations, such as magnetic domain walls, vortices, and staggered ferrimagnetic structures. The strength and orientation of the SMF are affected by the spatiotemporal change in magnetic structures, which are determined by the geometry and magnetic interactions within the sample [27, 28]. As previously mentioned, the exchange interaction of electrons with a mobile domain wall can lead to the creation of the SMF. Conversely, charge-spin inter-conversion may occur due to spin-orbit couplings [27, 28]. It can be deduced that the conversion between spin and charge, which arises from the Rashba and Dresselhaus spin-orbit interactions, is a consequence of spin and momentum coupling[29, 30]. Thus, the coupling of spin and momentum from various interactions, including that of Weyl semimetals and topological insulator (TI) materials, serves as the origin of the inter-conversion between spin and charge. SMF is typically determined through the unitary transformation method, where the non-collinear magnetic component of the Hamiltonian is transformed into a collinear diagonalizable effective Hamiltonian This technique has also been effectively utilized to compute the resistance of domain walls, showcasing its versatility and impact [31, 32]. Nevertheless, when both spin-momentum and exchange interactions are present, it is impossible to convert both of these two terms into a collinear effective system using just spin

rotation unitary transformation. In this research, we have proposed a unitary transformation applicable to such systems by reducing the dimensionality of the system, effectively removing the direction perpendicular to the electric field-driven current through an additional unitary transformation. This approach allows for the derivation of a diagonalizable Hamiltonian, and the unitary transformation method can be extended to include systems with spin-momentum coupling. This phenomenon emphasizes the complex relationship between magnetic dynamics and spin-dependent effects on conduction electrons[33]. In 1984 Berger on his pioneering studies revealed that electric current gives rise to motion in domain wall[34–36]. He declared that electric current applies a force on the domain wall via the exchange coupling[35]. Dynamics of domain wall under limited currents in the ferromagnets was investigated in[37] and it was showed that this current has two effects: first one that relates to the charge current and resistance of the wall is momentum transfer effect and the other is spin transfer effect that relates to the spin current [38]. Current induced domain wall dynamics in an antiferromagnetically coupled system was investigated by experimental and theoretical modeling methods[39]. It has been shown that the current induced domain wall motion reaches maximum at the angular momentum compensation point[39]. Moreover, it was revealed the interval structure of domain walls and the underling mechanisms for the fast domain wall motion. In the current work it was assumed that the domain wall motion is generated by the electric current inside the magnetic substrate and the dynamics of it's effective field has been experienced by the conduction electrons at the upper layer of the Weyl semimetal.

2 Berry phase and Generalized Faraday law

The Berry phase is an angular measurement that ranges from 0 to 2π, signifying the overall phase change of a state vector as it traverses a path in its parametric vector

space. This quantity also admitted as a "geometric phase"[40]. Berry's phase is characterized within the framework of electron behavior in periodic solids, and a particular expression is formulated to articulate it and presence of a nonzero Berry phase in one dimensional parameter space is declared by rare torus topology of Berillouin zone. The symmetrical nature of Bloch functions in the Brillouin zone leads to the quantization of Berry's phase. By linking Berry's phase to Wyckoff positions in crystals through the band representations of space groups, one can leverage Berry's phase to label energy bands in solids[41]. Faraday's Law indicates that the electromotive force (ε) is equal to the negative rate of change of magnetic flux (ϕ) with respect to time, represented by the equation $\varepsilon = -d\phi/dt$. In the context of ferromagnetic materials, this law is adapted to incorporate the effects of non-conservative spin forces. Rather than using magnetic flux (ϕ) directly, we substitute it with $\partial A/\partial t = \nabla \times A$, where A denotes the average Berry phase influenced by the directions of electron spins. These modifications guarantee the conservation of energy while the order parameter is changing of itinerant ferromagnets[42]. A proposed adjustment to Faraday's Law incorporates nonconservative spin forces through the generalized version of the law

$$\varepsilon = -\frac{\hbar}{(-e)}\frac{d\gamma}{dt} \tag{1}$$

In this relation, γ denotes the spin average of the Berry phase, which incorporates both the charge and spin of conduction electrons. The conventional model of an itinerant ferromagnet needs to be updated to include the Berry phase. The induced potential energy, labeled $\phi^{\pm}s$, differs for majority and minority electrons, represented by the upper and lower signs, respectively. In straightforward scenarios, $\phi^{\pm}s$ is defined as $\mp\mu B_i(r)$, where $B_i(r)$ indicates the strength of the position-dependent internal field. Additionally, it is crucial to understand that the force, $-\overrightarrow{\nabla}\phi^{\pm}s$, observed in the Stern-Gerlach experiment is conservative and does not affect the electromotive force (ε).

The spin Berry phase is represented as $\gamma^{\pm}s = \frac{1}{2}\int \overrightarrow{A^{\pm}s} \cdot dr$, where $\overrightarrow{A^{\pm}s}$ plays a role in the overall spin force, which is further described by the following relation [42]:

$$\overrightarrow{f^{\pm}s} = -\frac{\hbar}{2}\frac{\partial \overrightarrow{A}^{\pm}s}{\partial t} - \overrightarrow{\nabla} r\phi^{\pm}s \tag{2}$$

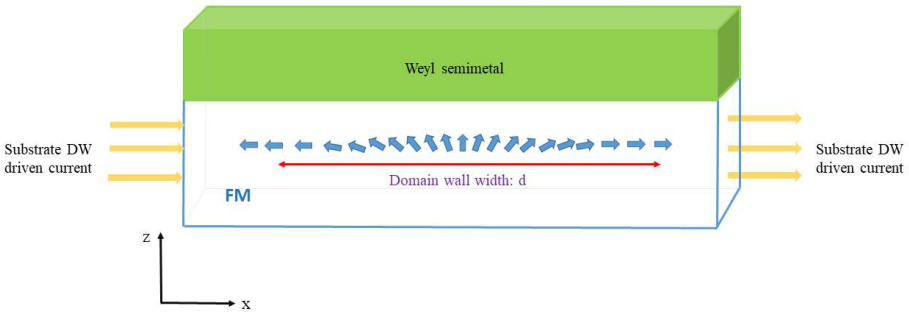


Fig. 1 Neel type magnetic domain wall at the substrate of the Weyl semimetal thin film.

3 RESULTS

Hamiltonian that describes the low energy electrons around the Weyl nodes is supposed in the form[43]:

$$H = sv_f(\vec{p}\cdot\vec{\sigma}) - J\vec{M}(\vec{r},t)\cdot\vec{\sigma} \tag{3}$$

where $s = \pm 1$ stands for chirality of Weyl nodes, v_f denotes Fermi velocity, σ is Pauli matrices and J is the strength of the exchange interaction between spin of conduction electrons of Weyl semimetal and magnetic substrate, $\vec{M}(\vec{r},t)$ is the induced

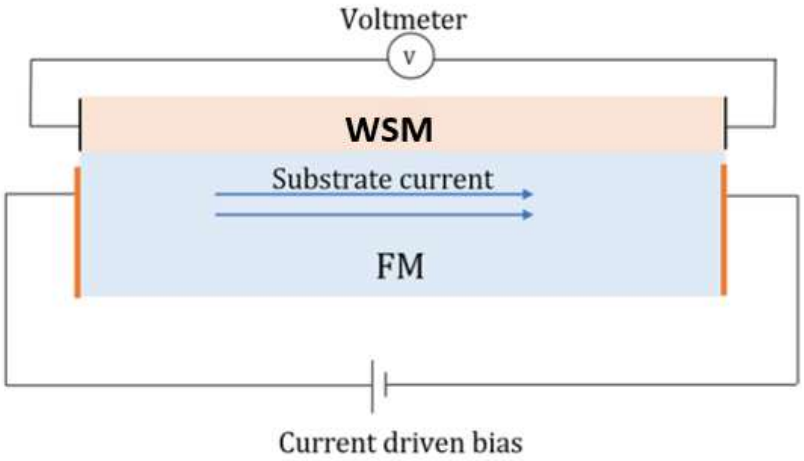


Fig. 2 Domain wall driven electric current at substrate of the Weyl semimetal thin film

magnetization of substrate. $\vec{p} = -i\vec{\nabla}$ stands for momentum operator and $\vec{M}(\vec{r}, t) = M\vec{n}$, where $\vec{n}$ shows the direction of the magnetization which characterizes with θ angle that local spins make with z axis. Spatial dependence of θ is:

$$\theta(x, t) = \arccos(\tanh \frac{x - x_0(t)}{d}) \tag{4}$$

where x_0 is the center of the wall and d stands for the width of magnetic domain wall. It is assumed that the substrate contains Neel type domain wall in which its rotation axis is x as shown in figure 1. Motion of domain walls driven by electric current can be achieved by recognizing that spin-polarized electrons passing through the domain wall encounter spin-dependent forces that cause their spins to realign. This spin realignment transfers angular momentum to the domain wall via the spin-transfer torque mechanism. As a result, the generated torque allows the electric current to move the domain wall[44].

It was supposed that the motion of domain walls driven by current in the underlying layer is responsible for the magnetization dynamics illustrated in figure 2. Magnetic field has not been used for magnetization dynamics, since it's evident that the magnetic

field, generated domain wall motion, can also affect the populations of majority and minority spins of conduction electrons. This can lead to additional effects alongside with the exchange interaction between conduction and local spins.

As a result, utilizing an electric field has been suggested for inducing magnetic dynamics, potentially allowing for more efficient control of magnetic states without changing the spin-dependent population of conduction electrons. By applying an electric field, we can selectively influence local spin dynamics, enhancing our understanding of spin interactions.

The exchange term of the Hamiltonian can be transformed into a collinear term using a unitary transformation $U_\theta = \exp(-i\theta(x)\sigma_x/2)$. However, since the spin-momentum coupling terms remain non-collinear after this transformation, a second unitary transformation U_λ is required to eliminate the transverse momentum components [45]. The detailed derivation of both transformations is provided in Supplementary Information, Section S1.

The resulting effective Hamiltonian of Weyl fermions reads:

$$H' = sv_f p_x \sigma_x + \frac{\hbar}{2}\frac{\partial\theta}{\partial x} - JM\sigma_z \tag{5}$$

In the case of smooth domain walls with a significantly large width denoted by d, θ can be approximated as a linear function of position. This can be derived using a Taylor expansion, leading to the expression $\theta(x,t) = \frac{\pi}{2} - \frac{x-x_0(t)}{d} + \frac{(x-x_0(t))^3}{3d^3} + \ldots$. It is crucial to emphasize that the linear approximation used to describe the spatial dependence of local magnetization up to the second term, consequently Hamiltonian comes to form $H = sv_f p_x \sigma_x - \frac{\hbar}{2d} - JM\sigma_z$ then energy eigenvalues are achieved:

$$E_\pm = \pm\sqrt{J^2M^2 + \hbar^2 k_x^2 s^2 v_f^2} \tag{6}$$

The wave functions are written

$$\psi''^{\pm}_{s,k_x} = \begin{pmatrix} \alpha^s_{\pm} \\ \beta^s_{\pm} \end{pmatrix} \tag{7}$$

where we have defined

$$\alpha^s_{\pm} = \frac{s v_f \hbar k_x}{\sqrt{s^2 v_f^2 \hbar^2 k_x^2 + (JM + E_{k_x\pm})^2}} \tag{8}$$

and

$$\beta^s_{\pm} = \frac{JM + E_{k_x\pm}}{\sqrt{s^2 v_f^2 \hbar^2 k_x^2 + (JM + E_{k_x\pm})^2}} \tag{9}$$

Applying the reversed transformations, the eigenfunctions of the original Hamiltonian and the subsequent Berry phase calculation are presented in detail in Supplementary Information, Section S2.

The Berry phase for each eigenstate, considering that the integration is computable on a closed route including the magnetic wall along the system, reads:

$$\gamma^{\pm} = -k_x L - (\alpha_{\pm}, \beta_{\pm})[\theta(L,t) - \theta(0,t)] \tag{10}$$

In which L is the dimension of system along the x direction. It is important to mention that because the magnetic structure varies only along the x-axis, we have $A^{\pm}_y = 0$. As a result, calculating the gauge-invariant Berry phase along a closed path can be simplified to the integral of $A^{\pm}_x$ over the x-axis. Furthermore, the spin-dependent

motive force, denoted as $\varepsilon^{\pm}$, is determined in the following way:

$$\varepsilon^{\pm} = -\frac{h}{e} \cdot \frac{d\gamma^{\pm}}{dt} \tag{11}$$

The total spin-dependent force is represented by $E_{SMF} = \frac{\sigma^{+}-\sigma^{-}}{\sigma^{+}+\sigma^{-}}\varepsilon^{+} = p\varepsilon^{+}$, [33], where $p = \frac{\sigma^{+}-\sigma^{-}}{\sigma^{+}+\sigma^{-}}$ denotes the polarization of spin and $\sigma^{\pm}$ stands for electrical conductivity of majority and minority of spins. Moreover, when the Fermi energy falls within the upper band width, the spin-motive force is generated solely by this band, and the entire lower band does not play a role in contributing to the spin-motive force. In the present scenario, when the lower band is completely occupied and the Fermi level is located within the width of the upper band, that results in $p = 1$. Supposing that the magnetic wall of substrate moves with velocity of v_D and dynamics of the wall is considered by $x_0(t) = v_D t$.

The detailed steps of the SMF integration over occupied states are provided in Supplementary Information, Section S3. The total spin-motive force is obtained by taking into account the occupied states of the band energy. At the limit of steady state, time scale $t \sim \frac{L}{v_D}$, the final expression of spin-motive force of system is as follows:

$$\varepsilon^{+}_{tot,s} = \frac{sE_f}{2\pi ed}\frac{v_D}{v_f}e^{-\frac{L}{d}} \tag{12}$$

A notable feature of the results obtained in this work is the dependence of the generated spin-motive force on the chirality of the Weyl semimetal bands. This dependence indicates that if the populations of electrons with opposite chiralities are equal, the net chiral spin-motive force produced by the system vanishes. Therefore, the necessary condition for obtaining a nonzero spin-motive force is the presence of a finite chirality polarization. Consequently, the spin-motive force can be regarded as a probe and an effective tool for measuring chirality polarization.

In other words, chirality polarization in Weyl semimetal systems is a prerequisite for the generation of the spin-motive force. It should be noted that chirality polarization can be induced or detected through various methods, such as optical techniques[46, 47] or by employing noncentrosymmetric ferromagnets[48]. Previous studies have also pointed out the influence of chirality on the Hall effect, which in turn can be utilized for chirality detection[49].

Concerning the structure of the gauge field, the entirety of the spin gauge field forms an SU(2) gauge field. As highlighted in earlier studies [50, 51] the spin gauge field consists of both adiabatic and nonadiabatic (off-diagonal) elements. It has been established that the adiabatic part of the spin gauge field generates the spin motive force, whereas the nonadiabatic component drives the spin pumping effect [50]. Additionally, at the adiabatic regime it has been demonstrated that the effective SU(2) gauge field simplifies to its adiabatic component, which is a $U(1)$ gauge field, sharing the same mathematical framework as electromagnetism [50, 51].

The theoretical basis for this differentiation is well-founded. In the adiabatic limit ($t \to \infty$), the off-diagonal components of the $SU(2)$ gauge field can be disregarded due to their rapid oscillation, characterized by $\exp(\frac{-it\triangle}{\hbar})$, $\triangle$ representing the excitation energy [50]. Similar findings in other research indicate that when the Hamiltonian, H, and the diagonalizing transformation U change gradually with respect to parameters, and their derivatives are minimal, the non-Abelian SU(2) gauge field transforms into an Abelian diagonal gauge field [51].

In the adiabatic approximation, the off-diagonal components of the gauge potential are ignored. As a result, the diagonal potential is treated as Abelian gauge, which causes the commutator term $[A_i, A_j]$ in the gauge field tensor to disappear [51]. This leads to the conclusion that, within the adiabatic limit, the separate eigenstates can evolve independently. Thus, the relevant U(1) component for calculations involving spin-motive force is the following expectation value $A^{\pm}(\vec{r}) = i < \psi_{\pm} \mid \frac{\partial}{\partial r} \mid \psi_{\pm} >$ [50].

4 DISCUSSION

4.1 Concluding remarks and limitations

In this study, the behavior of a magnetic substrate made up of two magnetic domains separated by a domain wall has been examined in the generation of spin-motive force (SMF) in a Weyl semimetal. To transform the non-collinear magnetic system into a collinear one, the gauge transformation method is utilized. This transformation can be performed analytically for systems that lack spin-momentum coupling. However, when spin-momentum coupling is present, the gauge transformation adds terms that involve spin rotation in real space, which makes the transformed system non-collinear and unsuitable for analytical diagonalization.

In present research, we first apply a gauge transformation to align the exchange interaction. Then by another unitary transformation which allows us to eliminate the position-dependent spin component of the Hamiltonian caused by the spin-momentum term. As a result, we obtain an equivalent Hamiltonian that can be analytically diagonalized, making it easier to calculate the Berry phase. Our findings indicate that the movement of the magnetic wall in the substrate can create an effective chirality dependent spin-motive force in a Weyl semimetal.

In the present study, SMF arises from the time-dependent Berry phase created by the substrate domain wall motion, according to the principles of generalized Faraday's law [42]. The energy of driving the SMF comes from the work done by the substrate current, which opposes damping forces to maintain the domain wall velocity, denoted as v_D. This energy is transformed through the interaction between exchange coupling and spin-momentum locking $sv_f(\vec{p} \cdot \vec{\sigma})$, leading to the emergence of nonequilibrium SMF on the surface of the topological insulator, in accordance with energy conservation principles where the work done by the external circuit is equal to the SMF energy and Joule heating. It is important to clarify that the electric field responsible for SMF discussed in this study is not an external field, but rather an emergent spin dependent

electric field produced through the spin gauge mechanism, as described in reference [50].

The spin-orbit coupling presented in the Hamiltonian of a Weyl semimetal leads to a complex Berry curvature. This curvature enables the movement of domain walls to generate a gauge field $A^{\pm}$, which directly results in the emergence of a SMF. This process illustrates how the magnetic dynamics of the domain wall, influenced by spin-momentum locking, interact with charge degrees of freedom, effectively demonstrating a dynamic inverse Edelstein effect [52]. In this effect, fluctuations in the spin texture are transformed into charge currents through the framework of an emergent spin gauge field.

Furthermore, the suggested approach is applicable to analogous systems featuring spin-momentum locking. The results indicate that the produced SMF is notably affected by both the size of the domain wall and its speed, which is propelled by the electric current in the substrate. Additionally, we have generalized the unitary transformation method to compute spin-momentum currents in systems that exhibit spin-momentum coupling.

According to the expression obtained for SMF, this quantity seems to be influenced by the dimensions of the system. However, when the limit is taken as $L \to \infty$, the SMF becomes less sensitive to the size of the system and eventually dissipates as time approaches infinity. In finite-size systems, where L is comparable to d, the system exhibits SMF with alternating signs, operating within a characteristic time scale of $\frac{d}{v_D}$, which diminishes the overall average SMF. In larger systems, the SMF also reverses sign over the same time scale.

It is important to note that the findings of this study pertain to situations where a constant velocity can be achieved, at least over a specific time period. Therefore, it is clear that the immediate accelerations of the domain wall are overlooked.

Our research indicates that a substantial SMF can be created in a non-equilibrium state due to the electric field that drives the motion of domain walls. The SMF is

associated with the width of the domain wall via $\frac{1}{d}e^{\frac{-L}{d}}$ and is directly proportional to the velocity of the wall. Consequently, regarding the local magnetic field, the SMF is more likely to emerge when the smooth domain walls are moving quickly.

This indicates that the domain wall must be large enough. Additionally, for sharp domain walls, it becomes impossible to meet the requirements of the adiabatic regime. The ideal situation for achieving a significant SMF happens when $L \sim d$. In an entirely non-adiabatic regime, characterized by extremely short domain walls, the $SU(2)$ formalism is applicable, but the reduced $U(1)$ gauge theory fails to capture the physics of the system.

4.2 SMF Enhancement mechanisms and experimental prospects

The magnitude and observability of the spin-motive force (SMF) have been extensively investigated in conventional magnetic systems. In ferromagnetic and ferrimagnetic materials, it has been shown that the emergent electromotive response arises from the adiabatic component of the SU(2) spin gauge field generated by time-dependent magnetic textures. In particular, it has been demonstrated that the SMF scales with the domain-wall velocity, magnetization gradient, and spin polarization [38], while its magnitude typically lies in the range of 10^2 nV to μV in experimentally accessible geometries [53]. Furthermore, it has been theoretically predicted that Rashba spin-orbit coupling can dramatically enhance the SMF [54]. It has been demonstrated that Rashba interaction introduces an additional spin-dependent gauge contribution, effectively amplifying the emergent electric field associated with magnetic texture dynamics. In systems with strong Rashba coupling, the induced electromotive force can exceed conventional estimates by orders of magnitude due to the coupling between real-space magnetization gradients and momentum-space spin-orbit fields

[54]. The present Weyl system shares key conceptual elements with both mechanisms, yet introduces a fundamentally distinct amplification channel. In contrast to ordinary ferromagnets, Weyl semimetals intrinsically host spin-momentum locking protected by band topology. The Weyl Hamiltonian $H = sv_f(\mathbf{p} \cdot \boldsymbol{\sigma})$ naturally generates a momentum-dependent spin texture, which acts as an intrinsic bulk analogue of Rashba-type spin-orbit coupling. Consequently, the emergent gauge field induced by magnetic domain-wall motion is not solely determined by exchange interaction but is strongly influenced by the chiral band structure. This intrinsic spin-momentum locking enhances the Berry-phase sensitivity of conduction electrons to magnetic texture dynamics. As a result, the chirality-dependent SMF derived in this work can benefit from mechanisms analogous to Rashba-induced amplification, particularly in magnetic Weyl semimetals or in ferromagnet/Weyl heterostructures where inversion symmetry breaking and interfacial electric fields further strengthen effective spin-orbit interactions. Therefore, from an experimental standpoint, the detectability of the predicted chirality-selective SMF can be improved. Importantly, while conventional ferromagnets generate SMF through spin polarization imbalance, the Weyl system requires finite chirality polarization to produce a non-vanishing net electromotive response. This distinction provides an additional tunable degree of freedom absent in ordinary magnetic metals. Therefore, the combination of topological band structure, intrinsic spin-momentum locking, and magnetic texture dynamics offers a promising pathway toward enhanced and experimentally accessible electromotive signals beyond standard ferromagnetic estimates.

5 METHOD

5.1 Theoretical Framework and Generalized Unitary Transformation

The primary challenge in calculating the spin-motive force (SMF) in systems with simultaneous spin-momentum coupling and non-collinear exchange interaction is the inability to diagonalize the Hamiltonian using a single standard spin-rotation unitary transformation. To overcome this, we propose a two-step generalized unitary transformation approach.

First, a spatially dependent spin-rotation operator, $U_\theta = \exp(-i\theta(x)\sigma_x/2)$, is applied to align the local magnetization of the domain wall along the collinear z-axis. While this successfully diagonalizes the exchange interaction term, the spin-momentum coupling terms acquire position-dependent non-collinear components. To resolve this, a second dimensionality-reduction transformation, $U_\lambda = \exp(i\lambda(p_y y + y p_y + p_z z + z p_z))$, is introduced. In the limit of large positive λ, this operator effectively suppresses the transverse momentum components (p_y, p_z), yielding a fully diagonalizable 1D effective Hamiltonian.

The complete mathematical derivations of these transformations, including the commutator expansions and the proof of transverse momentum suppression, are detailed in Supplementary Information, Section S1.

5.2 Berry Phase and SMF Evaluation

The SMF is evaluated using the generalized Faraday's law, where the emergent electromotive force is proportional to the time derivative of the spin-dependent Berry phase. The Berry connection is computed over a closed contour encompassing the magnetic domain wall. The calculation assumes the adiabatic regime, valid for smooth domain

walls ($d \gg$ lattice constant), where the non-Abelian $SU(2)$ gauge field reduces to an Abelian $U(1)$ gauge field.

The explicit evaluation of the Berry phase integrals, the application of the reversed transformations to the eigenfunctions, and the integration over the occupied Fermi sea to obtain the final macroscopic SMF are provided in Supplementary Information, Sections S2 and S3.

- Authors' contributions S. Ersi - Investigation, Conceptualization, Formal analysis & Writing-Original Draft. H. Mohammadpour - Supervising, Formal Analysis, Validation and Review. A. Phirouznia - Supervising, Methodology, Validation & Editing
- Data availability All data generated or analysed during this study are included in this published article and its supplementary information file.
- Conflict of interest The authors declare no competing interests.
- Funding Declaration This research received no specific grant from any funding agency in the public, commercial, or not-for-profit sectors.

References

[1] X. G. Wan *et al.*, Topological semimetal and Fermi-arc surface states in the electronic structure of pyrochlore iridates, Phys. Rev. B **83**, 205101 (2011).

[2] G. Xu *et al.*, Chern Semimetal and the Quantized Anomalous Hall Effect in $HgCr_2Se_4$, Phys. Rev. Lett. 107, 186806 (2011).

[3] Z. J. Wang *et al.*, Dirac semimetal and topological phase transitions in A_3Bi (A = Na, K, Rb), Phys. Rev. B **85**, 195320 (2012).

[4] S. M. Young *et al.*, Dirac Semimetal in Three Dimensions, Phys. Rev. Lett. **108**, 140405 (2012).

[5] Z. J. Wang *et al.*, Three-dimensional Dirac semimetal and quantum transport in Cd_3As_2. Phys. Rev. B **88**, 125427 (2013).

[6] H. M. Weng *et al.*, Weyl Semimetal Phase in Noncentrosymmetric Transition-Metal Monophos-phides, Phys. Rev. X **5**, 011029 (2015).

[7] S. M. Huang *et al.*, A Weyl Fermion semimetal with surface Fermi arcs in the transition metal monopnictide TaAs class, Nat. Commun. **6**, 7373 (2015).

[8] S. Y. Xu *et al.*, Discovery of a Weyl fermion semimetal and topological Fermi arcs, Science **349**, 613 (2015).

[9] B. Q. Lv *et al.*, Experimental Discovery of Weyl Semimetal TaAs, Phys. Rev. X **5**, 031013 (2015)

[10] L. X. Yang *et al.*, Weyl semimetal phase in the non-centrosymmetric compound TaAs, Nat.Phys. **11**, 728 (2015).

[11] Hosur, P. Qi, X. Recent developments in transport phenomena in Weyl semimetals Développements récents concernant les phénomènes de transport dans les semi-métaux de Weyl, C R Phys. **14**, 857 (2013).

[12] Wan, X., Vishwanath, A. Savrasov, S. Y. Computational design of axion insulators based on 5d spinel compounds, Phys. Rev. Lett. **108**, 146601 (2012).

[13] Z. Wang, S. C. Zhang, Chiral anomaly, charge density waves, and axion strings from Weyl semimetals, Phys. Rev. B **87**, 161107 (2013).

[14] S. Rao, Weyl semi-metals: a short review, arXiv:1603.02821 (2016).

[15] N. P. Armitage *et al.*, Weyl and Dirac semimetals in three-dimensional solids, Rev. Mod. Phys.**90**, 015001 (2018).

[16] J. Ieda, Y. Yamane and S. Maekawa, Spinmotive force in magnetic nanostructures, Spin. **3**, 1330004 (2013).

[17] S. A. Yang, G. S. D. Beach, C. Knutson, D. Xiao, Q. Niu, M.Tsoi, and J. L. Erskine, Universal Electromotive Induced by Domain Wall Motion, Phys. Rev. Lett. **102**, 067201 (2009).

[18] M. Hayashi, J. Ieda, Y. Yamane, J. I. Ohe, Y. K. Takahashi, S.Mitani, and S. Maekawa, Phys. Rev. Lett. **108**, 147202 (2012).

[19] K. Tanabe, D. Chiba, J. Ohe, S. Kasai, H. Kohno, S. E. Barnes, S. Maekawa, K. Kobayashi, and T. Ono, Spin-motive force due to a gyrating magnetic vortex, Nat. Commun. **3**, 845 (2012).

[20] S. Mühlbauer, B. Binz, F. Jonietz, C. Pfleiderer, A. Rosch, A.Neubauer, R. Georgii, and P. Boni, Skyrmion Lattice in a Chiral Magnet, Science **323**, 915 (2009).

[21] Y. Yamane, K. Sasage, T. An, K. Harii, J. Ohe, J. Ieda, S.E. Barnes, E. Saitoh, and S. Maekawa, Continuous Generation of Spinmotive Force in a Patterned Ferromagnetic Film, Phys. Rev. Lett. **107**, 236602 (2011).

[22] M. Nagata, T. Moriyama, K. Tanaka, D. Chiba, J.Ohe, Y. Hisamatsu, T. Niizeki, H. Yanagihara, E. Kita, and T. Ono, Spin motive force induced in Fe3O4 thin films with negative spin polarization, Appl. Phys. Exp. **8**, 123001 (2015).

[23] W. M. Saslow, Spin pumping of current in non-uniform conducting magnets, Phys. Rev. B **76**, 184434 (2007).

[24] R. A. Duine, Spin pumping by a field-driven domain wall, Phys. Rev. B **77**, 014409 (2008).

[25] Y. Tserkovnyak and M. Mecklenburg, Electron transport driven by nonequilibrium magnetic textures, Phys. Rev. B **77**, 134407 (2008).

[26] Y. Yamane, Spin-motive force due to domain-wall motion in the presence of Dzyaloshinskii-Moriya interaction, Phys. Rev B **98**, 174434 (2018).

[27] M. I. Dyakonov and V. Perel, Current-induced spin orientation of electrons in semiconductors, Physics Letters A **35**, 459 (1971).

[28] J. E. Hirsch, Spin Hall Effect, Phys. Rev. Lett. **83**, 1834 (1999).

[29] E. Ivchenko, Y. B. Lyanda-Geller, and G. Pikus, Photocurrent in structures with quantum wells with an optical orientation of free carriers, Soviet Journal of Experimental and Theoretical Physics Letters, **50**, 175 (1989).

[30] V. M. Edelstein, Spin polarization of conduction electrons induced by electric current in two-dimensional asymmetric electron systems, Solid State Communications **73**, 233, (1990).

[31] A. Phirouznia, M. M. Tehranchi, and M. Ghanaatshoar, Influence of Rashba coupling on the magnetoresistance of a smooth domain wall, Phys. Rev. B **75**, 224403 (2007).

[32] R. Majidi, M. M. Tehranchi, A. Phirouznia, and K. G. Tabrizi, Influence of longitudinal optical phonons on domain wall resistance in nanowires based on diluted magnetic semiconductors, Phys. Rev. B **83**, 035413 (2011).

[33] K. Tanabe and J. Ohe, Spin-Motive Force in Ferromagnetic and Ferrimagnetic Materials, Journal of the Physical Society of Japan **90**, 081011 (2021).

[34] L. Berger, Low-field magnetoresistance and domain drag in ferromagnets, J. Appl. Phys. **49**, 2156 (1978).

[35] L. Berger, Exchange interaction between ferromagnetic domain wall and electric current in very thin metallic films, J. Appl. Phys. **55**, 1954 (1984).

[36] L. Berger, Motion of a magnetic domain wall traversed by fast-rising current pulses, J. Appl. Phys. **71**, 2721 (1992).

[37] G. Tatara, H. Kohno, J.Shibata, Microscopic approach to current-driven domain wall dynamics, Physics Report. **468**, 213 (2008).

[38] G. Tatra, H. Kohno, Theory of Current-Driven Domain Wall Motion: Spin Transfer versus Momentum Transfer, Phys. Rev. Lett. **92**, 086601 (2004).

[39] S. A. Siddiqui, J. Han, J. T. Finley, C.A.Ross and L. Liu, Current-Induced Domain Wall Motion in a Compensated Ferrimagnet, Phys. Rev. Lett. **121**, 057701 (2018).

[40] D. Vanderbilt, Berry Phases in Electronic Structure Theory: Electric Polarization, Orbital Magnetization and Topological Insulators, Titolo collana (Cambridge University press, 2018).

[41] J. Zak, Phys. Rev. Lett. 62, 2747 (1989).

[42] S. E. Barnes and S. Maekawa, Generalization of Faraday's law to include nonconservative spin forces, Phys. Rev. Lett. **98**, 246601 (2007).

[43] Y. Araki and K. Nomura, Charge pumping induced by magnetic texture dynamics in Weyl semimetals, Physical Review Applied. **10**, 014007 (2018).

[44] A. Yamaguchi, T. Ono, S. Nasu, K. Miyake, K. Mibu and T. Shinjo, Real-Space Observation of Current-Driven Domain Wall Motion in Submicron Magnetic Wires, Phys. Rev. Lett. **92**, 077205 (2004).

[45] R. F. Mehrabani, B. Abdollahipour, H. Mohammadpour, and A. Phirouznia, "Generation of non-equilibrium spin-motive force at the surface of a topological insulator induced by current-driven domain wall motion in the magnetic substrate," Physica B: Condensed Matter, 419046 (2026).

[46] Z. Fan *et al.*, Versatile tunable optical injection of chiral polarized Weyl fermions in a magnetic Weyl semimetal Co3Sn2S2, National Science Review, **12**, Issue 12, December 2025, nwaf402

[47] C.K. Chan, N.H. Lindner, G.Refael and P. A. Lee, Photocurrents in Weyl semimetals, Phys. Rev. B. **95**, 041104(R), (2017).

[48] R. Ray *et al.*, Tunable chirality of noncentrosymmetric magnetic Weyl semimetals in rare-earth carbides, npj Quantum Materials, **7**, Article number: 19 (2022).

[49] S. A. Yang, H. Pan, F. Zhang, Chirality-Dependent Hall Effect in Weyl Semimetals, Phys. Rev. Lett. **115**, 156603, (2015).

[50] G. Tatara, Effective gauge field theory of spintronics, Physica E:Low-dimensional Systems and Nanostructures, **106**, 208 (2019).

[51] K. Y. Bliokh and Y. P. Bliokh, Conservation of Angular Momentum, Transverse Shift, and Spin Hall Effect in Reflection and Refraction of an Electromagnetic Wave Packet, Annals of Physics **319**, 13 (2005).

[52] W. Luo, W. Y. Deng, H. Geng, M. N. Chen, R. Shen, L. Sheng, and D. Y. Xing, Perfect inverse spin Hall effect and inverse Edelstein effect due to helical spin-momentum locking in topological surface states, Phys. Rev. B **93**, 115118, (2016).

[53] P. N. Hai, S. Ohya, M. Tanaka, S. E. Barnes, and S. Maekawa, Electromotive force and huge magnetoresistance in magnetic tunnel junctions, Nature **458**, 489 (2009).

[54] K.-W. Kim, J.-H. Moon, K.-J. Lee, and H.-W. Lee, Prediction of giant spin motive force due to Rashba spin-orbit coupling, Phys. Rev. Lett. **108**, 217202 (2012).

Supplementary Files

This is a list of supplementary files associated with this preprint. Click to download.

- ErsiScirepSupplementary.pdf